

**GRID GENERATION FOR
TWO-DIMENSIONAL FINITE
ELEMENT FLOWFIELD
COMPUTATION**

**KENNETH E. TATUM
MCDONNELL AIRCRAFT COMPANY
MCDONNELL DOUGLAS CORPORATION
ST. LOUIS, MISSOURI**

To facilitate development of the finite element method for fluid dynamics problems a 2-D mesh generation scheme has been developed with the emphasis on versatility and independence of the finite element solution algorithm to be employed. No effort has been expended to maintain grid line orthogonality since the finite element method has no such requirement. The method consists of sequences of shearings and conformal maps with upper

and lower surfaces handled independently to allow sharp leading edges. The method will generate meshes of triangular or quadrilateral elements. Thus, with certain additional constraints of smoothness and near-orthogonality, a quadrilateral mesh could be generated for a finite volume type method. Finally, solutions obtained by the MCAIR finite element full potential flow program on sample meshes are shown to illustrate their usefulness.

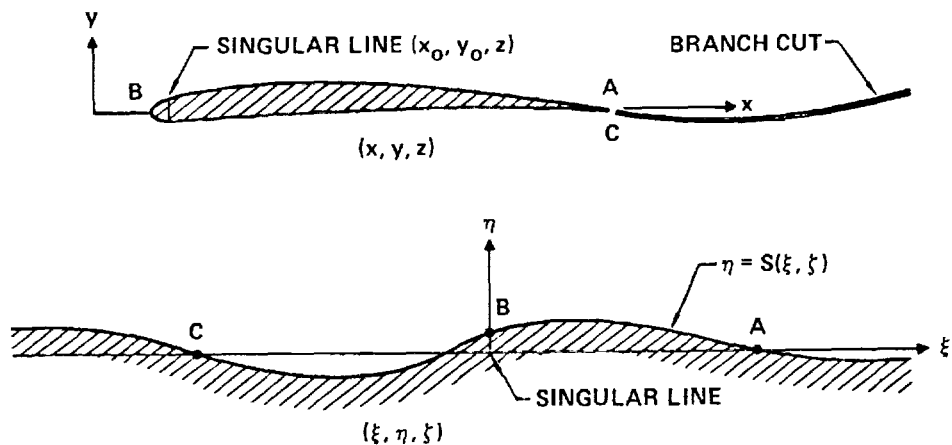
TYPICAL ANALYTIC TRANSFORMATION PARABOLIC PLUS SHEARING

The parabolic transformation shown is a typical method used to generate body fitted coordinate meshes for 2-D flowfield computations. Precise transformation Jacobians must be defined relating the uniform cartesian computational grid to the physical body-conforming coordinate grid. Computations are performed by Finite Difference Methods (FDM) in the cartesian coordinate space with determinants of the Jacobians appearing as added coefficients in the difference equa-

tions. Simple analytic transformations, even if multiple, cause little increase in complexity of the equations. However for complex body shapes numeric transformation techniques must be employed requiring Jacobian matrices to be computed for each grid cell. These matrices, often approximated, must be stored within the computer or recomputed for successive iterations of nonlinear systems. Either technique is costly.

$$\xi = i\eta = \left\{ [x - x_0(z) + iy - iy_0(z)] / t(z) \right\}^{1/2}$$

$$\zeta = z$$



AND THE SHEARING TRANSFORMATION

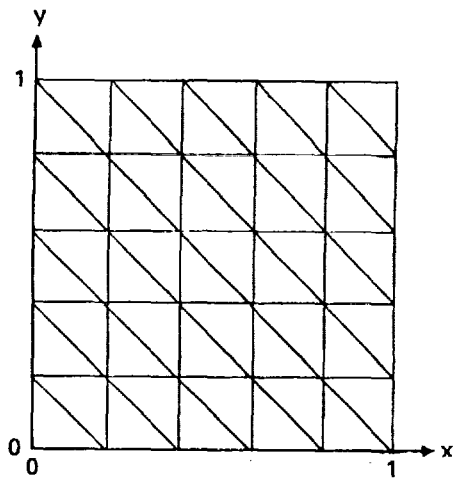
$$X = \xi \quad Y = \eta - S(\xi, \zeta) \quad Z = \zeta$$

Figure 1

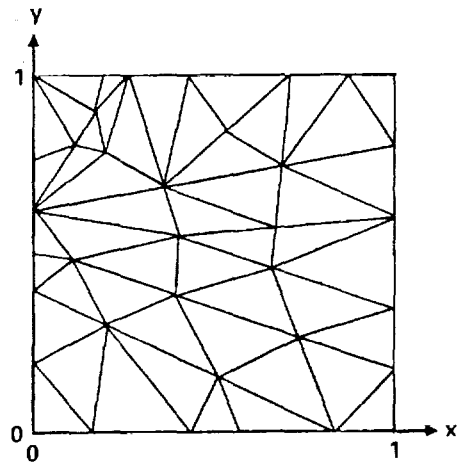
POSSIBLE FINITE ELEMENT MESH TRIANGULATION ON UNIT SQUARE

McDonnell Aircraft Company (MCAIR) is studying the Finite Element Method (FEM) as a method which might eliminate, or drastically reduce, the cost associated with transformation Jacobians. The FEM is equally suited to uniform cartesian meshes or irregular, highly non-orthogonal meshes. Two distinctly different FEM meshes (triangulations) of the unit square are shown in Figure

2. Each mesh contains 36 nodes and are equally usable even though a specific problem may indicate the desirability of one over the other. Computations may thus be performed directly in physical space on body-fitted grids generated independently of orthogonality constraints. Only the physical nodal coordinates and the relationships of nodes to elements must be stored.



36 NODES
50 ELEMENTS



36 NODES
48 ELEMENTS

Figure 2

COMPLEX SINE CONFORMAL MAPPING

Grid generation for a FEM computation may be performed by many means. While conformal mappings of simple, highly regular grids are not necessary from the standpoint of maintaining orthogonality, they are useful in producing grids with simple relationships between nodes and elements. Accordingly the current MCAIR technique is based on a conformal (sine) mapping of a rectangular

region to a semi-oval region. A sequence of shearing and stretching transformations both prior to and subsequent to the conformal mapping, shape line E'F'A' to that of one surface of the airfoil, either upper or lower. The number of, or localization of, the shearings is entirely unimportant as long as they may be programmed easily.

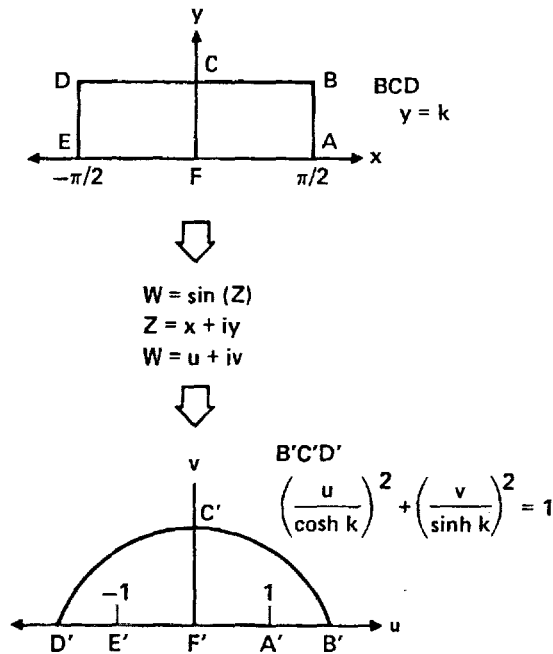


Figure 3

MATCHING OF UPPER AND LOWER MESH REGIONS

The general method described by Figure 3 is used twice to form two mesh regions as shown in Figure 4, one about the upper surface and one about the lower surface. The airfoil is situated with the forward-most and aft-most points at $y = 0, x = \pm 1$ and the two regions are designed to match along the line

$y = 0, |x| \geq 1$. Points along the line AC are doubly specified thus creating a cut across which wake/circulation boundary conditions may be applied. Points along the matching line BD are merged and no boundary is considered there in the final mesh.

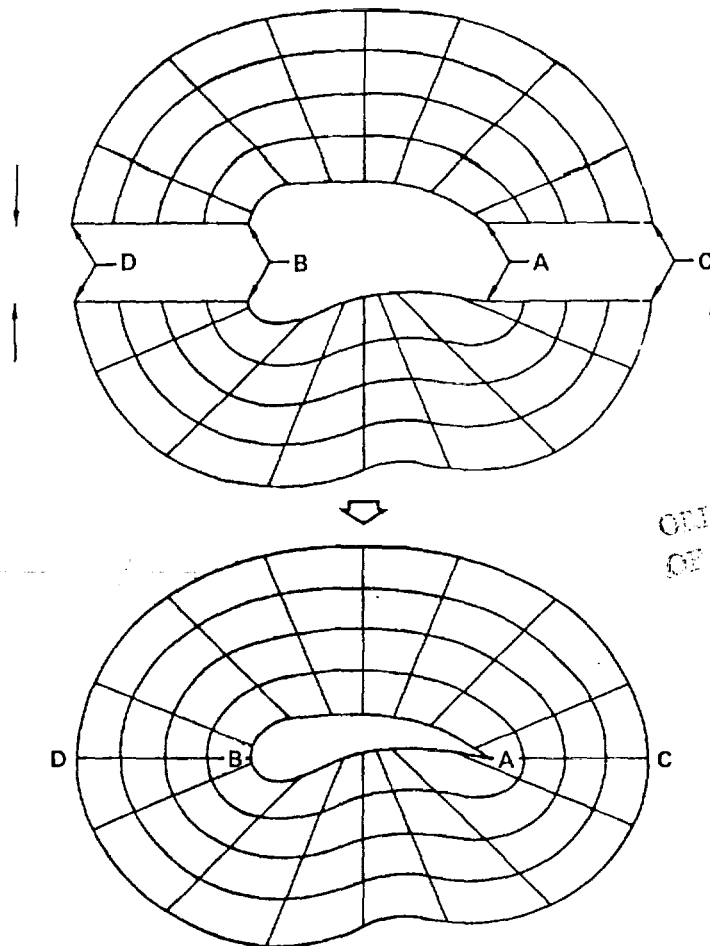


Figure 4

TRIANGULATION OF FIELD BY DIVIDING QUADRILATERALS ALONG APPROPRIATE DIAGONAL

The actual computation of nodal coordinates has been automated in a Fortran computer code for an arbitrary airfoil either specified analytically or by discrete points. Program inputs allow the exact specification of the desired mesh spacing along the body surface as well as the relative spacings normal to the surface. The final field is triangulated as shown in Figure 5 by dividing quadrilaterals along a diagonal, with the

diagonal direction varying between regions of the mesh in such a way as to prevent the conformal map from collapsing a triangle to zero area. Triangular elements are desired only because of the simplicity of finite element integration over such regions. However, if desired, quadrilateral elements are obviously generated quite as readily by the scheme.

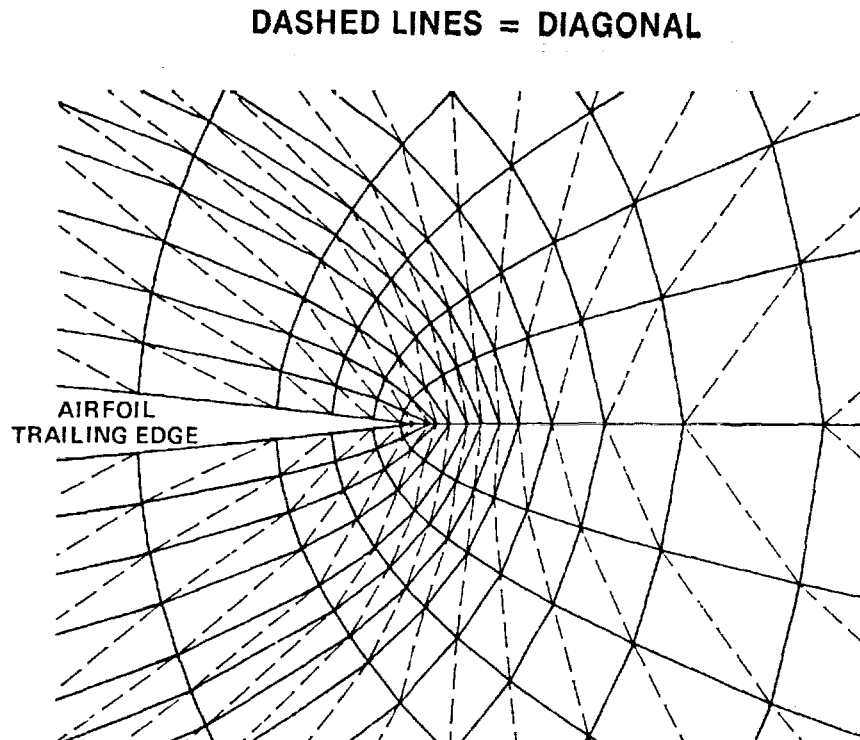


Figure 5

16.3% NLR 7301 AIRFOIL

72 x 17 MESH

Figure 6 shows a final resultant mesh generated about a modern supercritical airfoil, the 16.3% thick NLR 7301 airfoil, with the coordinate system scaled by the airfoil chord. The mesh consists of 72 elements bounding the airfoil surface with

17 rows of elements extending outward from the surface. A total of 1314 nodes define the 2448 elements. Neither the bluntness of the leading edge region nor the reverse curvature of the aft lower surface create any difficulties for the method.

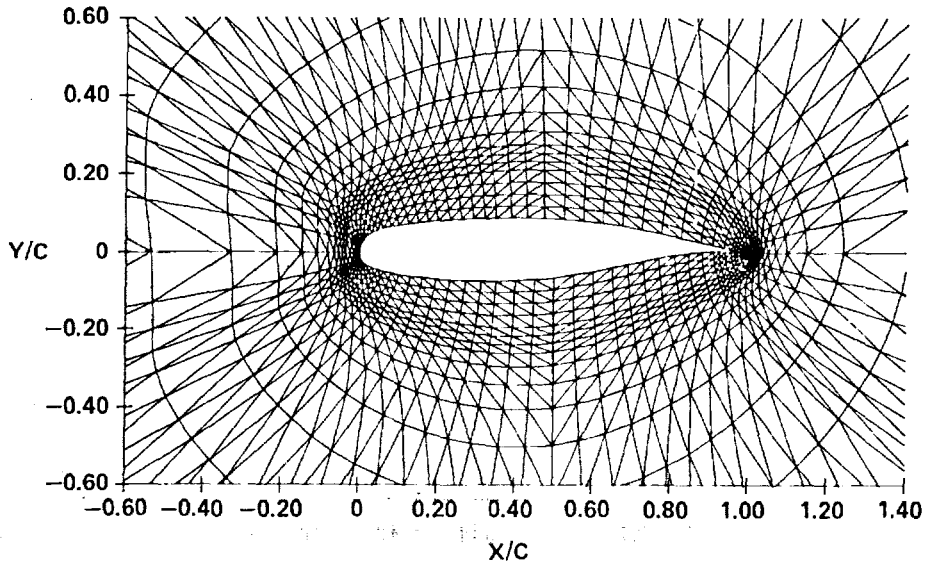


Figure 6

6% SYMMETRIC BICONVEX AIRFOIL

72 × 17 MESH

Figure 7 shows a sample mesh about an airfoil with opposite extremes to that of Figure 6. The airfoil is a thin (6%) symmetric Biconvex section with sharp leading and trailing edges. The sharpness of the leading edge presents no difficulties for the method due to the independent handling of upper and

lower surfaces. No singular point (x_0, y_0) , as needed for example by the parabolic transformation illustrated in Figure 1, exists for this type of leading edge. Thus, any solution procedure depending on a singularity point unwrapping transformation will fail on this airfoil.

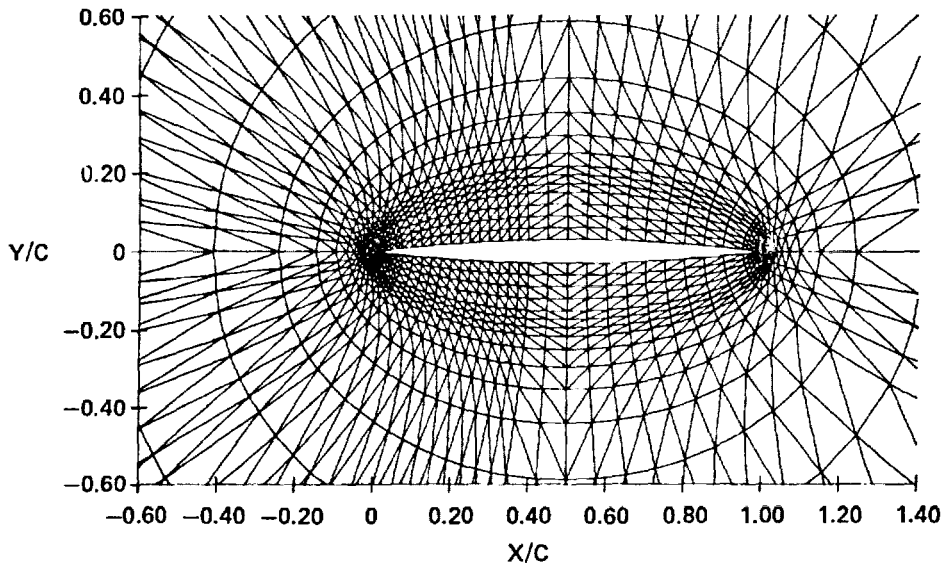


Figure 7

6% SYMMETRIC BICONVEX AIRFOIL LEADING EDGE

Figure 8 is an enlargement of the leading edge region of the mesh in Figure 7. Some local stretchings of the mesh have been automatically performed by the computer code to prevent some elements from becoming too small or thin. The stretchings may distort the smooth variation of elements around the leading edge but in reality increase the potential for obtaining an accurate finite element solution on the mesh

due to the maintaining of smaller aspect ratios (maximum/minimum dimension of triangle) of individual elements. Another constraint on the elements necessitating some local stretching is that the magnitude of the area of the smallest element not be too small relative to significant digit resolution of the computer on which calculations are to be performed.

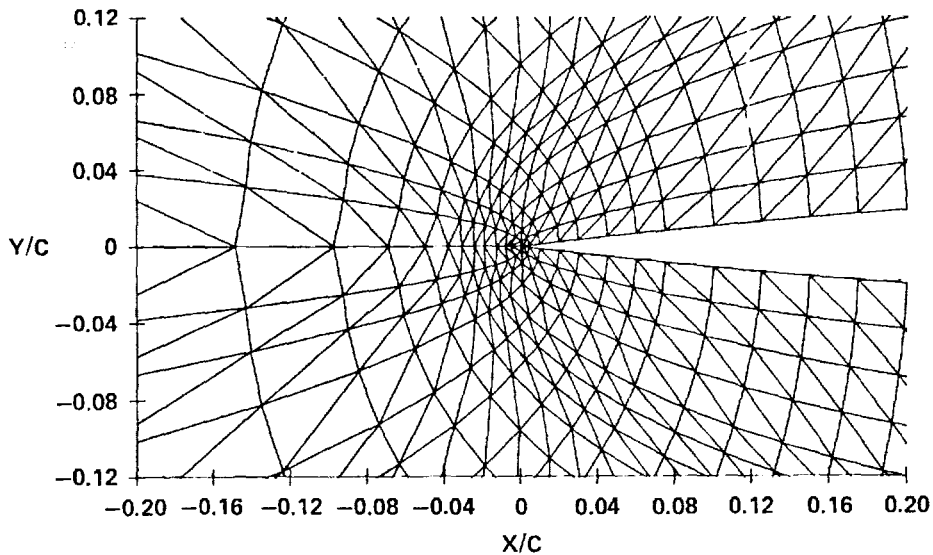


Figure 8

SUPERSONIC FIGHTER AIRFOIL (20° AND 10° FLAPS)

72 × 17 MESH

The use of shearing transformations not restricted to maintaining orthogonality of the grid allows the creation of grids about sharp corners. Figure 9 shows a grid about a supersonic fighter airfoil section with both leading and trailing edge flaps deflected. The discontinuous surface slopes at the hinge lines might create numerical singularities in

methods which attempt to maintain orthogonal grids. The MCAIR technique however has no such difficulties. The computer program also allows element spacings to be user specified to facilitate bunching of elements around the flap hinges where high velocity gradients are to be expected in the FEM solution.

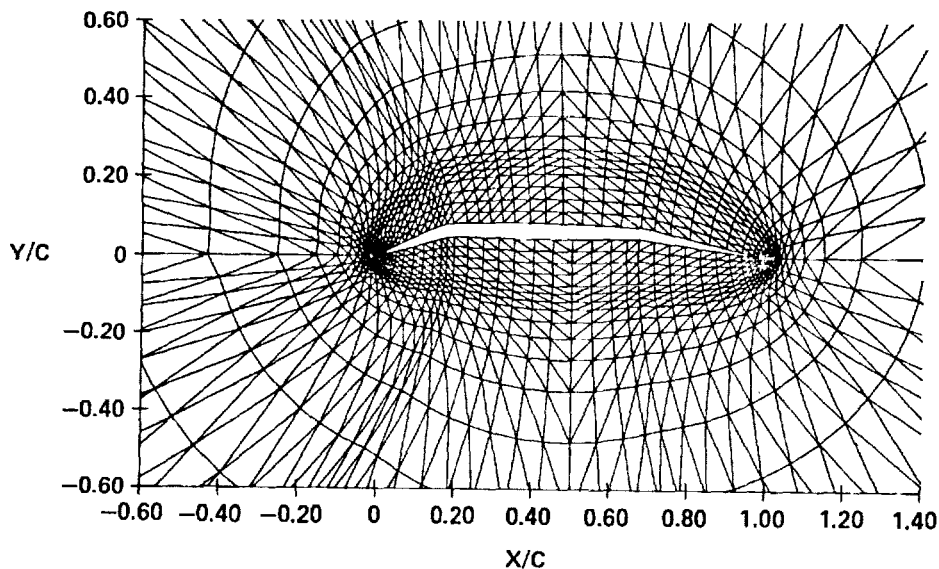


Figure 9

NLR SYMMETRIC SHOCK-FREE AIRFOIL

36 × 17 MESH

Figure 10 is an example of a half-plane mesh about a symmetric NLR shock-free airfoil design. The independent handling of upper and lower airfoil surfaces allows this type of mesh to be generated very simply. Flow solutions about symmetric airfoils at zero angle-of-attack may thus be obtained at half the expense or with double the nodal density but no additional cost. Such

solutions are important in fundamental research and also for comparison of full potential flow solutions with small perturbation solutions. These small perturbation solutions are most strictly valid at small, or zero, angle-of-attack on thin or sharp nosed airfoils such as the biconvex section shown in Figure 7.

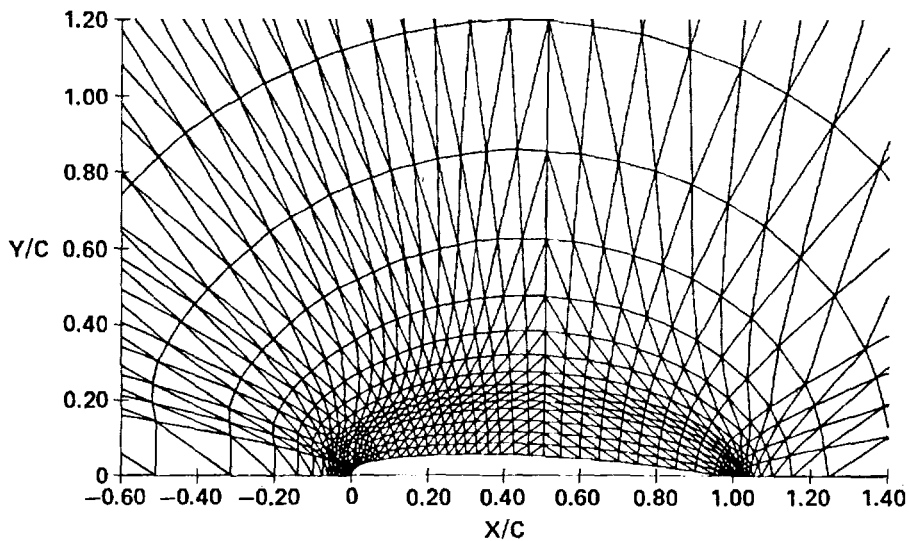


Figure 10

16.3% NLR 7301 AIRFOIL

ALPHA = 0.391° MACH 0.502

Figures 11-13 illustrate the use of the meshes shown in previous figures by the current MCAIR FEM full potential flow program. Figure 11 compares a FEM solution at a moderate subsonic Mach number (0.5) and

small angle-of-attack to the solution by a modern state-of-the-art Finite Difference Method (FDM) program. The comparison is good even though the FDM grid was much denser than the FEM mesh.

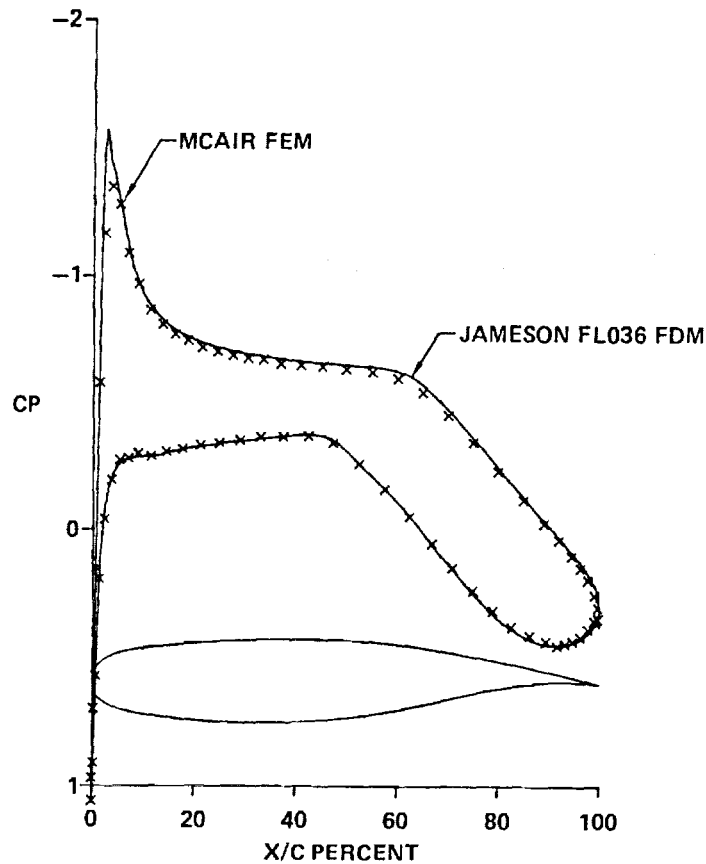


Figure 11

ORIGINAL PAGE IS
OF POOR QUALITY

SUPERSONIC FIGHTER AIRFOIL (20° AND 10° FLAPS)

ALPHA = 1.0° MACH 0.5

Figure 12 compares solutions for the supersonic fighter airfoil with 20° leading edge and 10° trailing edge flaps. Since no finite difference program was available which would compute flows about sharp leading edges and abrupt hinge lines, a modern technology Panel Method program, the Bristow Multielement Airfoil Analysis and Design (MAAD) program, was employed for

comparison. A Karman-Tsien compressibility correction was applied to obtain a Mach 0.5 solution. Agreement is good even in regions of pressure spikes; however, the inexpensive panel method employed approximately double the panel (solution node) density of the FEM and was able to more accurately resolve the pressure peaks.

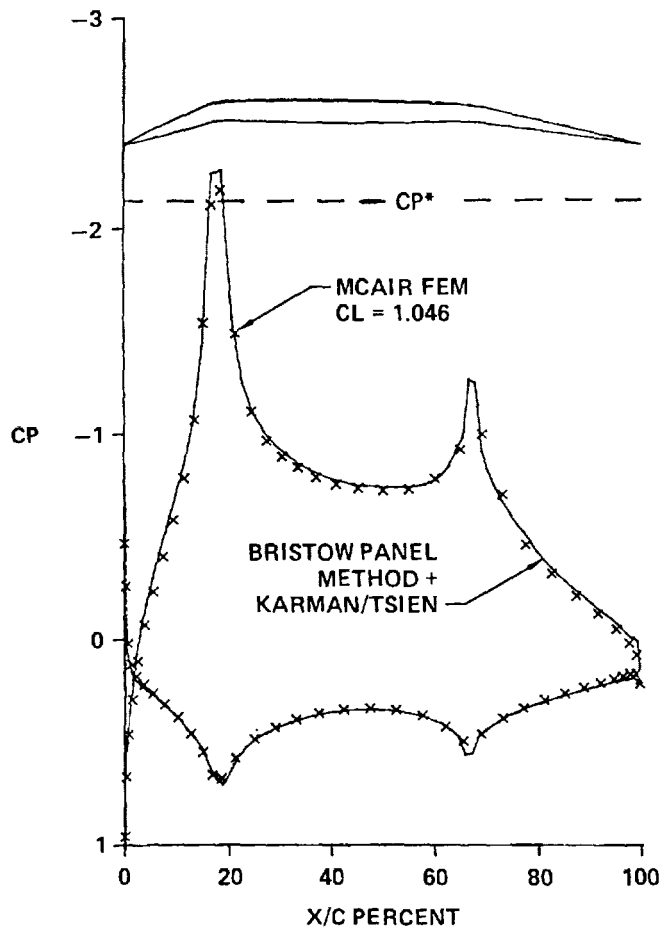


Figure 12

NLR SYMMETRIC AIRFOIL

ALPHA = 0° MACH 0.786

Figure 13 illustrates the use of a half-plane mesh, specifically that shown in Figure 9. The solution was obtained in the fundamental research on adapting the FEM to non-subsonic flowfields where the governing differential equations are of mixed elliptic/hyperbolic type. Using the artificial density concept of Holst the MCAIR FEM was

able to produce this solution on a shock-free airfoil which agrees reasonably well with the theoretical hodograph solution. The versatility of the mesh generator, both in technique and program, greatly facilitates the FEM research into fundamental computational methods and in applied fluid mechanics.

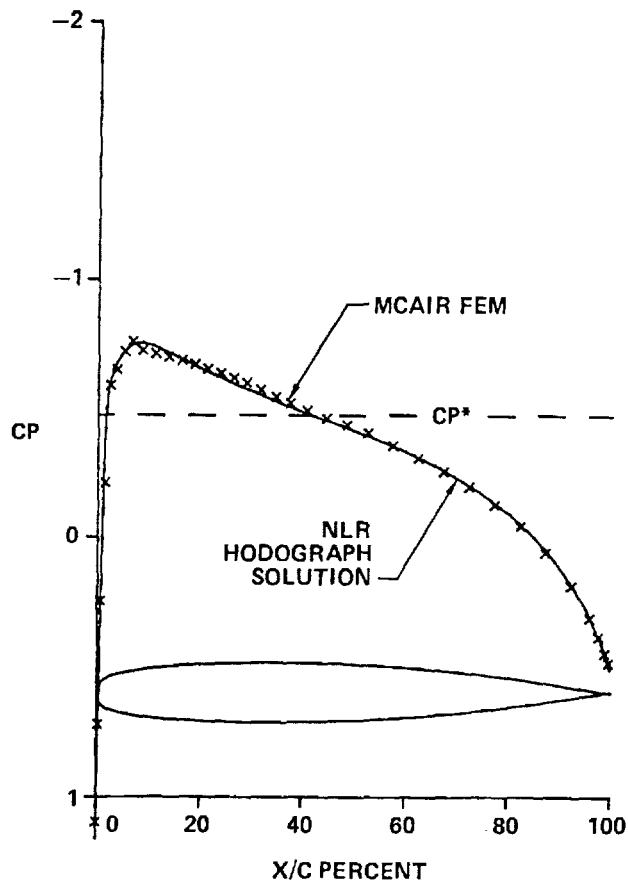


Figure 13